Experimental Study of the Fire Behaviour on Flat Roof Constructions with multiple Photovoltaic (PV) panels

Experimental Study of the Fire Behaviour on Flat Roof Constructions with multiple Photovoltaic (PV) panels

Abstract

Fire experiments were conducted on four mock-up roof constructions with an array of 6 Photovoltaic (PV) panels to study the fire dynamics and flame spread behaviour, so as to better characterise the fire risks of such a system. As it is customary to retrofit PV panels to existing warehouse roofs, where expanded polystyrene (EPS) and polyvinylchloride-based roofing membrane $B_{ROOF}(t2)$ is a typical roofing, the experiments were carried out on such installations, but with a mitigation solution on top; 30 mm mineral wool or 40 mm polyisocyanurate (PIR). All mock-ups were 6.0 m long, whereas the width was 2.4 m (Experiments 1 and 2) and 4.8 m (Experiments 3 and 4), respectively. A wood crib was placed under the PV panels and it ignited the roofing membrane after 7-8 minutes, which in all four experiments resulted in fire spread under all the six PV panels covering an area of $5.1\ \text{m} \times 2.0\ \text{m}$. However, no self-sustained fire was observed beyond the area below the PV array. Within the first hour, the maximum temperatures were measured to respectively 175°C and 243°C underneath the two mitigation solutions of PIR insulation and mineral wool, which is more than 100°C below the piloted ignition temperature for the EPS insulation. However, the EPS was ignited in both experiments with the PIR insulation due to thermal degradation of the protective material after approximately one hour. These experiments confirm that a small initial fire underneath a PV installation can transform into a hazardous scenario due to the changed fire dynamics associated with adding the PV panels to the existing roof.

Keywords: Photovoltaic panels, Fire Experiments, Fire Dynamics, Mitigation

1. Introduction

The rapid increase of energy produced globally by photovoltaic (PV) installations continued in 2017, with an increase of almost 100 GW, to a total of 402.5 GW [1]. In the US, an increase of 127 MW was made solely by three shopping malls and a real estate company [2], indicating a solid commercial interest in on-site PV power. A 58% price drop since 2012 [3] and protection from changing energy costs, are reasons for the increased popularity of the PV installations. Flat roofed buildings, such as warehouses or industrial production buildings, are particularly suitable for PV installations due to their large area and the fact that they are often elevated above the surrounding environment and thus capable of utilising the full potential of the installation.

However, the addition of PV installations, and thereby large electric systems powered by an energy source that cannot be turned off (the sun), introduces a new hazard that few buildings have been designed for. In Italy alone, 800 PV related fires occurred in 2012, after which it decreased to 600 and 469 fires in the following two years due to changed regulations [4]. Cancelliere [5] created a good overview of the issues related to the installation of PV arrays, where especially sections dealing with the cause of ignition and the propagation of the fire are of interest. The consensus seems to be that electrical malfunctions cause the initial fire on the roof constructions [6, 7, 8, 9]. Grant [10] described seven PV related fires in the US that all occurred due to electrical malfunctions, but he writes that the cause of the initial fire could also occur due to: (1) an external exposure fire, (2) fire originating within the structure, or (3) a fire originating in the PV system. From a fire safety engineering point of view, PV arrays installed on flat roof constructions are probable for both cause 1 and 3, but the consequences of both scenarios are similar - a fire developing underneath or in the PV installation. With an uncertainty of the power of a possible short circuit it would be of limited interest to test a specific set-up, since the difference between ignition and no ignition for a controlled short circuit also depends on the many surrounding factors - the fire often occurs due to the wrong events at the wrong time. Despite the uncertainty of the ignition source the fires occur and therefore the following experiments and analysis will focus on the propagation of the fire in case of an ignition underneath a PV array placed on a flat roof construction.

Backstrom and various co-authors carried out a series of projects at Underwriters' Laboratories, where they, based on UL1703 and UL790, tested how the introduction of PV panels or benchmark tests with non-combustible panels influenced the classification of different roof coverings [11-13]. The project focused on domestic installations on sloped roofs and how to prevent the installation to influence an existing fire [14]. They measured the maximum temperatures and heat fluxes and compared it with the critical heat flux for various roofing materials [14], and they came up with, and tested different mitigation solutions to prevent the fire from propagating underneath the panels [15-17].
Cancelliere and Liciotti [18] compared the reaction to fire for four different PV backsheets by the use of the Italian standards UNI 8957 and UNI 9174. The four backsheets obtained respectively the best and second best reaction to fire rating on a scale with five steps. Likewise, recent parametric studies [19] have showed that the PV panel itself only contains a limited amount of combustible materials such as a thin polymer based backsheet and combustible encapsulate materials. When ignited, the materials increase the heat flux towards the subjacent roof surface for a very short period because of the thin combustible layers and thereby limited time of combustion [19]. Given these points, the importance of the combustible materials in the main PV panel might be insignificant with respect to the propagation of the fire, - not to be mistaken with the fact that the PV panels probably are the main cause for the ignition, which leads to the fire.

Furthermore, the same recent parametric studies of the reflection of fire-induced heat underneath photovoltaic arrays [19] have shown that the reflected heat, combined with the deflected flame, represents an additional heat source that increases the total heat flux towards the roof construction significantly. It was found that the additional heat resulting from the PV panel could make the difference between whether or not the initial fire could spread beyond the ignition area.

Only a limited number of large-scale tests involving PV panels have been conducted. Backstrom and Dini tested the reaction to fire of three different types of PV systems (PV with glass front and aluminium frame, PV laminate and PV tiles) installed on a sloped roof [20]. In all these experiments, the roof constructions were uninsulated and the fire originated from the inside of the enclosure below the roof construction with PV panels (i.e. not in proximity of or in direct relation to the PV panels). As such, the objective was not to understand how the PV installation affected the fire, but rather to study how the fire affected the PV installation and their production of power. As a result, the findings were primarily of relevance for the safety of firefighters.

In contrast, the experiments presented herein are the first study of fire spread underneath a multi-panel PV array, and the first experiments conducted on a realistic mock-up of a *flat roof construction with different roofing solutions*. The experiments are of relevance for the general understanding of PV related fires, and in particular for all stakeholders placing PV panels on flat roof constructions. More specifically, the main purpose of the current full-scale experiments was to verify an observation from fire events [21-22], namely that the installation of a PV array increases the area to which the fire propagates on a given substrate, most often to the entire surface area underneath the PV panels.

As many installations are currently retrofitted on top of an existing roof constructions (as complete re-roofing is not an option), and because the existing insulation material often is combustible, the introduction of a mitigation layer between the existing roofing and the PV panels has become a common solution. Therefore, the current experiments were designed to study: (1) If and how the fire would propagate underneath the PV arrays. (2) Whether or not the fire propagates outside the array. The tests were based on an existing roof construction insulated with expanded polystyrene (EPS) insulation, as this is a common roofing solution for warehouses, and because it was considered a worst-case scenario, given the flammability properties of EPS. In order to establish whether or not ignition of the EPS (existing roofing solution) could be avoided, different mitigation solutions were tested. Initial experiments without the mitigation layer showcased the combustibility of the EPS insulation in a similar setting [23], and 'baseline experiments' with only the EPS and the membrane was deemed unnecessary, as the entire assembly would go up in flames, even without the PV panels being present. For solutions with a mitigation layer, however, it was not expected that a sustained fire could be established outside the PV arrays due to the lack of the additional heat flux from re-radiation associated with the PV panels.

Because all four experiments were based on a set-up with one PV array, and not multiple arrays, it was not possible to study the spread of fire from one array to another. In such a case it would be of interest to study potential correlations between wind speed, wind direction, distance between arrays and potential spread of fire from array to array, as wind does indeed influence fires. Herein, however, it is very important to distinguish between the two terms *flame spread rate* and *flame spread* when it comes to the wind influence, as the terms, respectively, describe the velocity of the flame front (m/s) and the area of damaged roof construction (m^2). The extent of the wind influence varies for the two cases – with or without PV panels installed.

In open space (i.e. without PV panels), the wind influences several aspects of the fire propagation. For example, the flame spread rate increases as a function of concurrent flow [24] and decreases for opposed flows [25]. In both cases, the wind deflects the fire from the flame front resulting in either an increased or decreases heat flux towards the virgin fuel. As a result, the extent of flame spread can be reduced in the opposed flow direction and increased in the concurrent flow direction.

For the second case, that is, when a PV installation is introduced above the existing roof construction, a semi-enclosure is established close to the roof surface. The PV panels can then be compared to an inclined ceiling, which causes deflection and extension of the flames, where the extension depends on the angle of inclination and the heat release rate [26]. Qui et al. concluded that the flame extension beneath a confined ceiling is decreased as a function of an increased wind flow [27], something that in turn can change the fire dynamics. As the PV panels themselves change the fire dynamics, it is difficult to separate the two effects without an extensive parametric study with very controlled wind conditions. Such a study was not undertaken herein, but some comments about the wind and the wind influence are made in the experimental setup section and the results section, respectively.

To reiterate, a detailed understanding of how the wind affects the flame spread rate underneath PV installations would have required parametric studies and was not the objective for the current experiments. Rather, the objective was to study how a PV array influences the fire spread on a flat roof surface. In particular, the focus was on the extent of the fire spread underneath and outside of the PV panel array. In addition, the study focused on the downward spread through different roofing solutions.

2. Experimental set-up

The experimental set-up is divided into a description of the ignition source and a description of the four mock-ups used for the experiments.

2.1 Source of ignition

Although most PV related fires are assumed to occur due to an electrical malfunction, it was decided to ignite each mock-up by the use of a wood crib to ensure a similar source of ignition in all four experiments. The cribs were made of medium-density fibreboard (MDF) sticks with the dimension of $16\ \text{mm} \times 16\ \text{mm} \times 160\ \text{mm}$ and a heat of combustion of $18.4\ \text{kJ/g}$. Each wood crib consisted of six layers with four sticks and was constructed according to McAllister [28], whose equations were also used to calculate the maximum theoretical heat release rate (HRR) of $30\ \text{kW}$ for the cribs. An experimental HRR was determined by measuring the mass loss rate of four wood cribs. Two of the wood cribs were tested on a non-combustible surface, whereas the other two wood cribs were tested on top of the two mitigations solutions to screen if they influenced the mass loss rate, which was not the case.

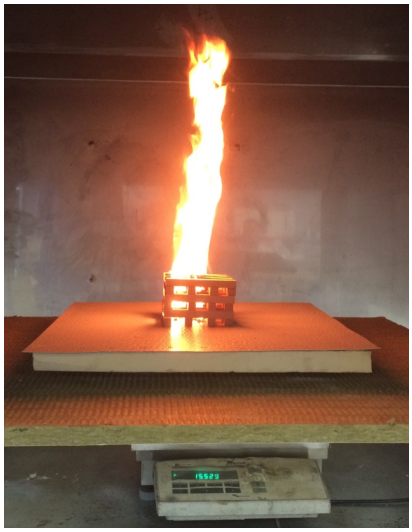

Figure 1 – Measurement of mass loss rate of the wood crib. From bottom to top: Scale, Mineral wool for protection of the scale, 40 mm PIR insulation, PVC-based roofing membrane, and wood crib.

2.2 Design of the mock-ups

A total of four full scale experiments were performed and the two kinds of mitigation layers were tested, see Table 1. All the mock-ups used for the experiments consisted of three components, as seen in Fig. 2; The existing roof construction, a mitigation solution, and vertical protection preventing ignition of the roof construction from the side of the mock-up. All of the roof constructions were built on top of a simple wood frame that made it possible to move each mock-up. The existing roof construction consisted of a self-supporting metal sheeting, 150 mm EPS insulation and a $B_{ROOF}(t2)$ classified polyvinylchloride-based (PVC-based) roofing membrane with a critical heat flux, q_{crit}, of 6.6 kW/m^2 [23]. The European classification $B_{ROOF}(t2)$ is based on the test method EN 1187 and the classification EN 13501-5.

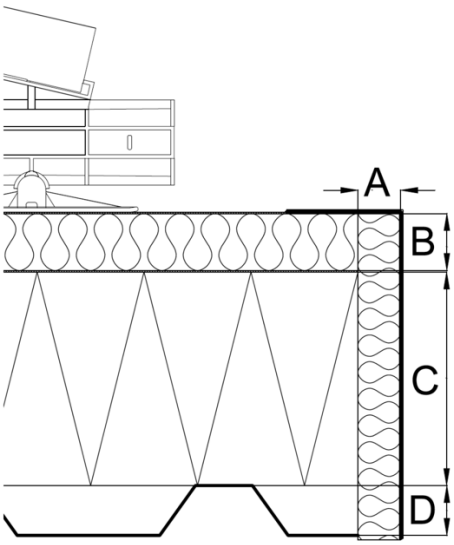

← Figure 2 - Sectional view of the roof construction underneath the PV installation. A: Vertical protection layer of 30 mm mineral wool fastened with a 1 mm metal sheeting. B: The mitigation layer and a layer of PVC-based roofing membrane. The mitigation layer for each test can be seen in tab. 3.1. C: Insulation on the existing roof construction - 150 mm EPS insulation with a layer of PVC-based roofing membrane. D: Self-supporting metal sheeting with a height of 35 mm. Parts of the used mounting system and a PV panel can be seen on top of the construction.

A mitigation solution was placed on top of the existing roof construction to prevent ignition of the EPS insulation. The mitigation solution consisted of a mitigation layer and an additional layer of the aforementioned roofing membrane. Initially it was decided to conduct the full-scale tests with two different types of mitigation layers: PIR insulation and mineral wool. Because the PIR insulation was manufactured with a layer of alufoil on each side of the product, a comparison of the temperature development underneath the two products was made in experiments where the samples were exposed to an identical external heat flux. A layer of roofing membrane and each of the mitigation products were placed inside a cone calorimeter sample holder and a type-k thermocouple was placed underneath the

insulation material. The samples were exposed to 20 kW/m^2 via the cone heater from a cone calorimeter and the temperatures were monitored as a function of time. Because the polyisocyanurate (PIR) insulation was manufactured with alufoil on both sides to decrease the influence of radiative heat towards the foam, the obtained temperature was significantly lower, as seen from Fig. 3. To make the PIR and the mineral wool more comparable from a pure heat transfer perspective, a third test with mineral wool and alufoil was conducted and resulted in a temperature reduction of around 150°C (Fig. 2).

Because of the temperature reduction accomplished by introducing the alufoil, a total of three different mitigation solutions were tested (Table 1). For the full-scale the experiments, it was decided only to test materials that were commercially available (in Denmark), which is the reason for the different thicknesses of the two mitigation layers. All layers were mechanically fixed by the use of 32 mm metal discs and 6 mm self-tapping screws.

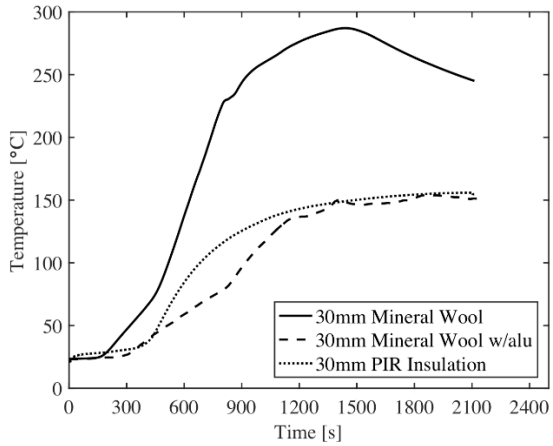

Figure 3 – Development of temperature underneath three different mitigation solutions exposed to 20 kW/m^2

Table 1 - Overview of the four test set-ups respectively mineral wool (MW) and polyisocyanurate (PIR) insulation.

Test #	Area of mock-up	Mitigation material	Wind
T1	2.4 m x 6.0 m	40 mm PIR	None
T2	2.4 m x 6.0 m	30 mm MW w/alu ♠	None
T3	4.8 m x 6.0 m	40 mm PIR	Mild
T4	4.8 m x 6.0 m	30 mm MW	Mild

♠: With a layer of alufoil on top of the mineral wool.

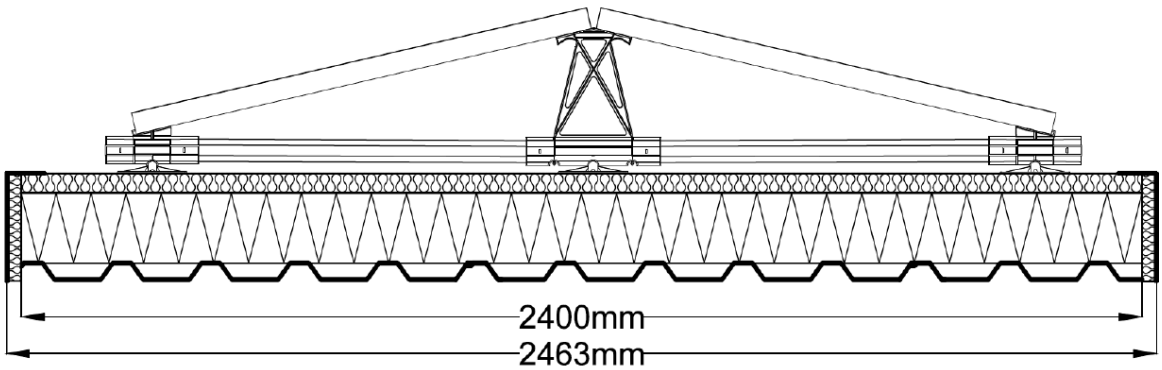

Figure 4 - Sectional cut of experiments T1 and T2. Experiments T3 and T4 were identical except from the width of the roof construction.

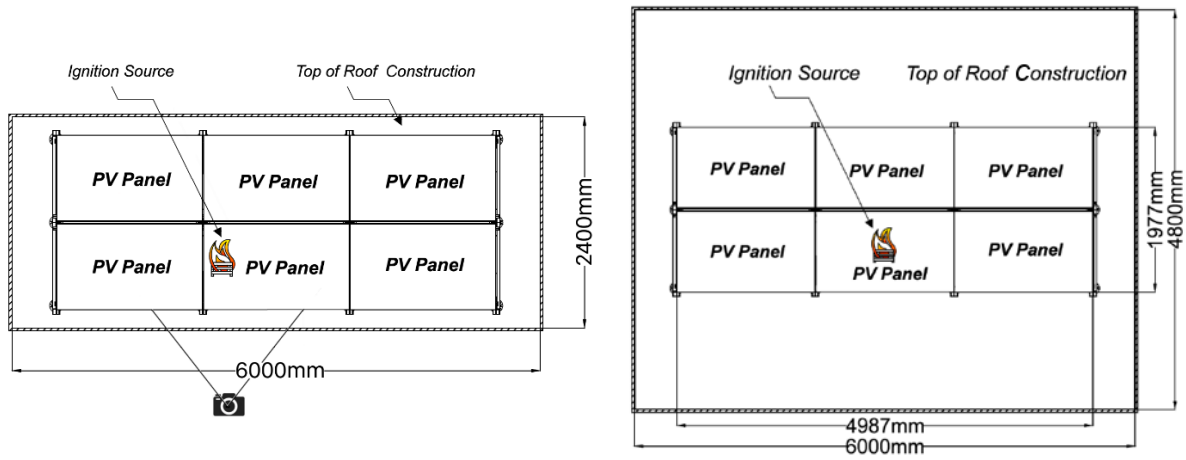

a) T1 and T2. The ignition source was placed underneath the junction box of the PV panel.

b) T3 and T4. The ignition source was placed underneath the centre of the PV panel.

Figure 5 – Top view of the two different experimental setups. The drawings are not to scale and the ignition sources are larger than the actual size.

The four experiments were conducted on two different days, resulting in slightly different weather conditions, as seen in Table 1. As the wind was not expected to affect the *flame spread* underneath the PV installation significantly, and because studying the *flame spread rate* was outside the scope of the current objectives, the wind speed was not monitored in detail in any of the experiments. However, an average wind speed on the days with experiments were reported at nearby weather stations. The values given were 1.9 – 3.2 m/s and 1.3 – 4.3 m/s, respectively.

Six fully functional PV panels, each with the dimensions of 1.7 m × 1.0 m, were installed in the centre of all four mock-ups as seen from the three drawings in Figs. 4 and 5. The PV panels consisted of a 3.2 mm thick tempered glass plate, poly-crystaline cells, a plastic backsheet and a 40 mm aluminium frame. The commercial available mounting system used for the installation of the PV panels was made of aluminium beams and plastic supports elevating the PV panels 320 mm in the centre and 90 mm on each side of the array. Where the main purpose of the first test round (T1 and T2) was to examine whether the fire propagated underneath the PV array, it was also possible to test if the fire propagated outside the array in the second test round (T3 and T4) where the area of the mock-ups were doubled as seen from Table 1 and Fig. 5.

Thermocouples were installed underneath the second layer of roofing membrane, on top of the EPS insulation and thereby in-between the two components of layer C in Fig. 2. In the first test round (T1 and T2) the thermocouples were placed along a horizontal and a vertical line intersecting underneath the point of ignition. In experiment T3 and T4, the temperature underneath the mitigation layers were measured with 20 type-K thermocouples located as shown in Fig. 6.

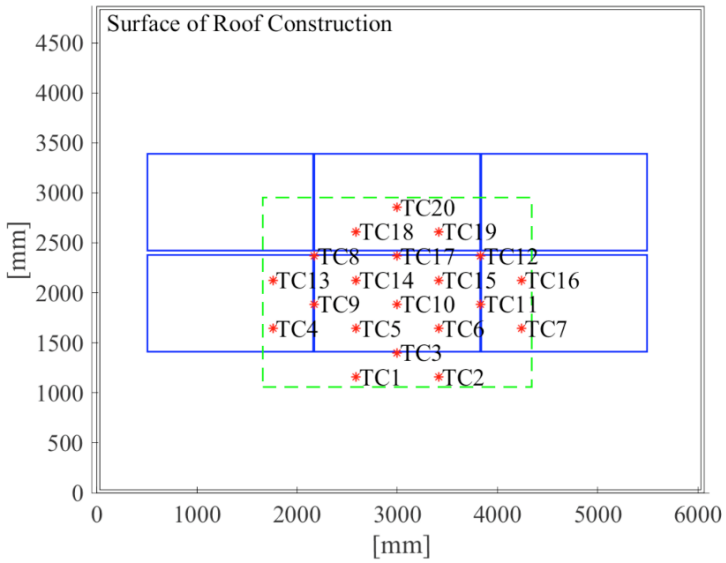

Figure 6 - Top view of the position of thermocouples (TC#) in experiment T3 and T4. The six blue squares mark the position of the PV panels. The dotted green line defines the view used in Figs. 13 and 14.

3. Results

3.1 Source of ignition

The four measurements of the mass loss rate did not reveal any significant difference between the experiments made on top of a non-combustible material, and the two mitigation solutions T3 and T4. Based on the mass loss rate (MLR) for the four experiments, a maximum steady state heat release rate (HRR) of 23 kW was calculated. Because of the re-radiation from the PV panels, the combustion efficiencies of the wood cribs are unknown. The stated HRR is therefore conservatively taken as the theoretical maximum based on the MLR, the heat of combustion for wood, and a burning efficiency of 100%. In addition, the experiments also constituted another important observation. The two separated mitigation solutions are shown in Fig. 7 and it can be seen that neither the roofing membrane nor any of the mitigation materials were affected by the heat from the ignition source outside a diameter of approximately 200 mm. The relatively small area affected, compared to the side length of the wood crib, indicated that the critical heat flux for flame spread across the roofing membrane used for the experiments was higher than the heat flux created by the wood crib alone. Thus, under normal circumstances (i.e. without PV panels), a fire of this size would not spread across the roofing membrane on top of PIR or mineral wool.

Figure 7 - Two of the mass loss experiments were carried out with a 0.60 m by 0.60 m section of a mitigation solution with a mitigation layer of either mineral wool (upper left) or PIR insulation (upper right) and the roofing membranes (front). An area with the width of approximately 1/3 of the total width was affected by the wood crib fire in all four experiments, defining the domain/distance where the heat from the wood crib can ignite the surrounding construction materials.

3.2 Full Scale Experiments – initial propagation

Despite the different wind conditions and the slight modification of the position of the ignition source, as seen in Fig. 5, the initial ignition of the roof construction occurred almost similar in all four experiments. Figure 8 shows the relevant frames of the ignition phase from experiment T2, where the wood crib was placed underneath the junction box and thereby next to the mounting system's transversal aluminium beam. As seen from Fig. 8 a, the limited amount of wind resulted in only vertical propagation of the fire inside the wood crib and no horizontal flames along the top of the roof construction. In the following frames in Figs. 8 b to d, it is seen how the heat from the wood crib ignited an object underneath the backside of the PV panel, whereupon the object dropped towards the top of the roof construction and ignited the roofing membrane. In Fig. 8 e the continuing fire indicates that self-sustained flame spread is established. From Figs. 8 f to h the fire propagates to a total of approximately 0.5 m along the right side of the roofing membrane, which after the propagation continued below the rest of the PV panel.

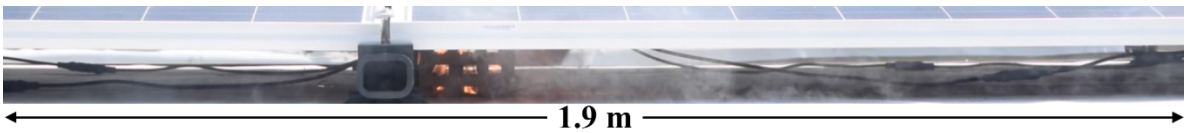

a) Time: 6:56 (frame 5 of 60), no ignition of membrane.

b) Time: 6:56 (frame 6 of 60), ignited material drops on right side of wood crib, below edge of PV panel.

c) Time: 6:56 (frame 7 of 60), ignited material continues to burn before it hits the membrane.

d) Time: 6:56 (frame 8 of 60), the falling, burning material ignites the roofing membrane.

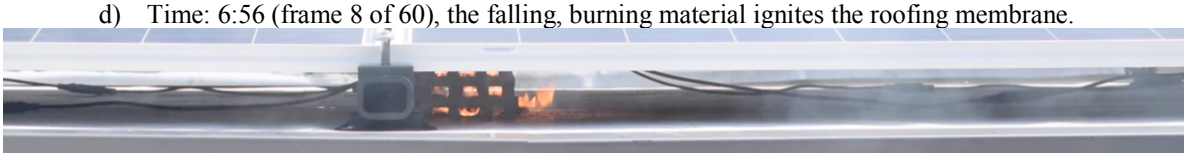

e) Time: 07:06, the fire is self-sustained.

f) Time: 07:21, the fire propagates towards the right side.

g) Time: 07:27, the fire propagates further towards the right side.

h) Time: 07:53, the fire ignites the cables underneath the panels.

Figure 8 - The ignition of the roofing membrane and initial propagation of the fire from experiment T2. The time is given in (min:s). The position of the wood crib and the viewpoint of the camera can be found in Fig. 4a.

Based on the video recordings of experiments T1 and T2, the distance between the flame fronts and the centre of the wood crib was estimated as a function of time from ignition of the wood crib, as seen in Fig. 9. For the two experiments, no spread occurred outside the source of ignition within the first 7 minutes, as the fire within the wood crib had to build up. This observation alone provides strong evidence for the crucial influence that the PV panels have on the fire dynamics and spread. The delay of approximately 3 minutes between the spread towards right side of the wood crib for test T1 and T2, occurred due a wind flow towards the left side of the picture in experiment T1. However, the inclination of the four plots in Fig. 9 are identical and equivalent to a spread rate of approximately 0.2 m/min.

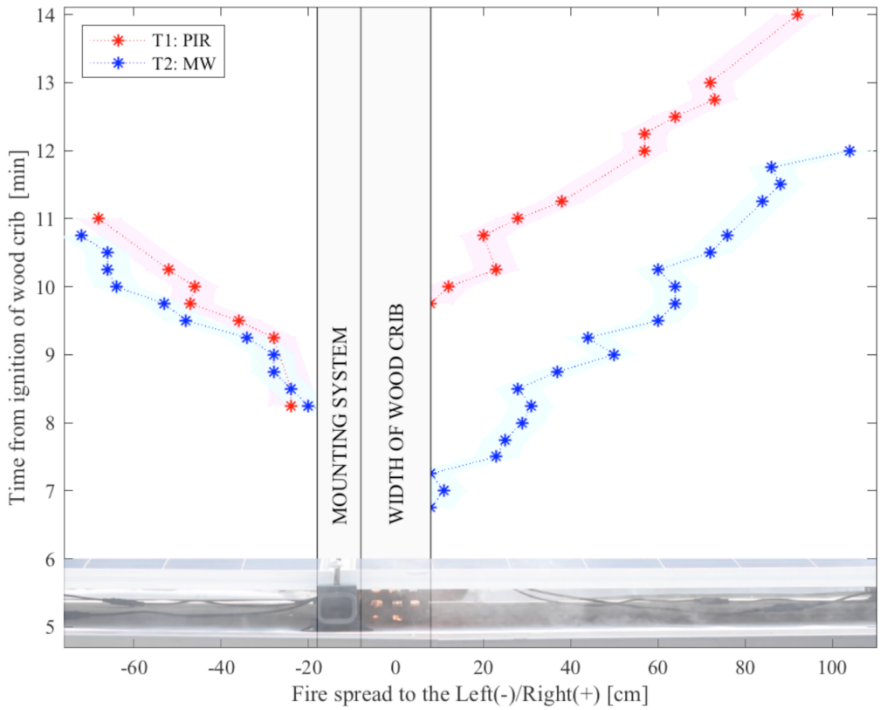

Figure 9 – Spread of fire as a function of time from ignition of the wood crib for experiment T1 (PIR) and T2 (MW). The fire did not spread beyond the ignition crib until around 7 minutes after ignition. The shaded areas

indicate an uncertainty of ± 50 mm. The position of the flame fronts were measured at the first frame for every 15 seconds, unless the view was obstructed by smoke. Please notice the swapped x- and y-axis.

3.3 Area of propagation

The fire propagated underneath all six PV panels in all four experiments, as seen from experiment T3 in Fig. 10, which also shows the maximum spread of the fire outside the array. Experiments T1 and T2 showed that the fire hardly propagated outside the array, which was in line with the laboratory experiments with just a crib (Section 3.1). However, due to the limited size of the mock-ups, it was not possible to eliminate the influence of possible adverse edge effects that could reduce the growth of the fire near the edges. The increased area of experiments T3 and T4 made it possible to examine how the fire propagated outside the array. The maximum spread distance outside the array was approximately 1 m, as seen from the picture in Fig. 10 and the two sketches in Fig. 11. The charred area in the left side of Fig. 10 shows the affected roofing membrane. The propagation outside the array did not occur due to propagation of the fire along the roofing membrane, but due to a wind-related deflection of the largest flames from the fire underneath the array.

When flames underneath a PV panel are deflected by wind, one can expect an increase in the heat flux towards the subjacent roofing membrane [19]. However, this increased heat flux will target a smaller area of the fuel, and it is unclear what effect it will have on the flame spread rate. Still, the extent of flame spread (i.e. not the rate) is not expected to be significantly altered by the wind, as these two wind-affected parameters in the system (smaller flame extension and higher local heat flux) will counteract each other. Finally, once the flames leave the area below the PV panels, the case will be that of open flame spread, as described above, and the extent of flame spread can be reduced in the opposed flow direction and increased in the concurrent flow direction. The experiments confirmed that the side of the PV panel array with opposed flow flame spread indeed had slightly lesser extent of flame spread than the side with concurrent flow. Still, the differences were minimal for the normal wind speeds present in the current experiments, and the current data does not support quantitative relations on the effect that wind may have on the extent of fire spread beyond the edge of the panel array.

Whereas the main PV panels did not contribute with a significant fuel load to the roof construction, all the plastic supports from the mounting system were ignited and burned until the fire were actively extinguished, as seen in Fig. 10.

The influence of the PV installation is thereby in accordance with the small scale laboratory experiments conducted by Kristensen et al. [23], which showed that the critical heat flux for spread could be reached with panels in place, but not without.

Figure 10 - Experiment T3. The whole area underneath the PV array was affected by the fire. Contrary to the picture, the dominant wind direction was from the right towards the left side of the picture as seen in Fig. 10 a.

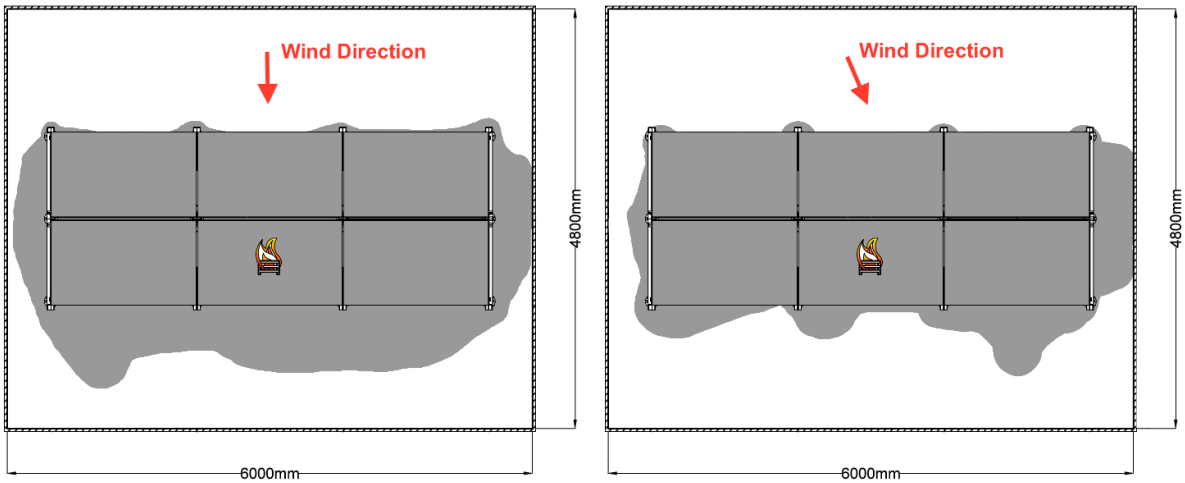

a) Experiment T3 with a mitigation layer of polyisocyanurate (PIR) insulation.

b) Experiment T4 with a mitigation layer of mineral wool (MW).

Figure 11 – Extent of fire propagation. The gray area indicates the roofing membrane affected by the fire.

3.4 Damage of the mitigation solutions

Although the different mitigation layers had no direct influence on the combustion of the top roofing membrane, it was seen that the mitigation layers reacted differently to the heat from the burning membrane and the wood crib.

In both experiments with a mitigation layer of PIR insulation (T1 and T3) it was seen that the heat from the wood crib compromised the integrity of the product, resulting in a penetration of the mitigation layer as seen in Fig. 12. Upon penetration of the PIR insulation, the findings strongly suggest that the EPS below was ignited. This is supported by the sooted EPS insulation and melted carbonised areas in Fig. 14 a, as well as by smoke observations during the experiments. Further support for this comes from the temperature data presented in Section 3.5. The three areas with melted EPS insulation, marked by red arrows in Fig. 14 a, developed due to the heat from the burning plastic supports.

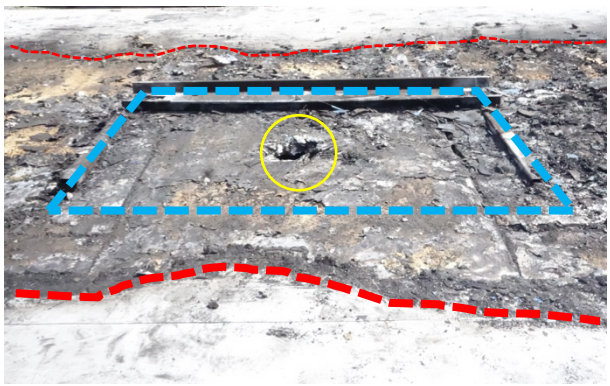

Figure 12 – Experiment T3. Part of mock-up cleared from leftovers and PV panel. Approximate width of the picture at centre: 1.8 m. Yellow circle: penetrated PIR insulation at the point of ignition. Blue square (stippled lines): position of PV panel above point of ignition. Red stippled line: indicates the edge of the roofing membrane.

Figure 13 – Experiment T4. Part of mock-up cleared from leftovers and PV panel. Approximate width of the picture at centre: 1.2 m. Yellow circle: Point of ignition without penetration of the mineral wool.

In the two experiments with a mitigation layer of mineral wool (T2 and T4) there were no physical damage of the mitigation layer, as seen from Fig. 13, which thereby separated the fire from the EPS insulation that were not ignited in both experiments. In spite of the non-ignited EPS insulation, it was still affected by the conductive heat transfer through the mineral wool, which melted the EPS. The damaged areas of EPS insulation were strongly dependent on whether the additional layer of alufoil was placed above the mineral wool. In experiment T2 only a circular area with a diameter of approximately 1 m was melted away, whereas most of the area underneath the PV array was affected in experiment T4, as seen from Fig. 14 b. In both experiments with a mitigation layer of mineral wool there was no sign of fire or combustion in the EPS insulation since there was no sooty or carbonised areas.

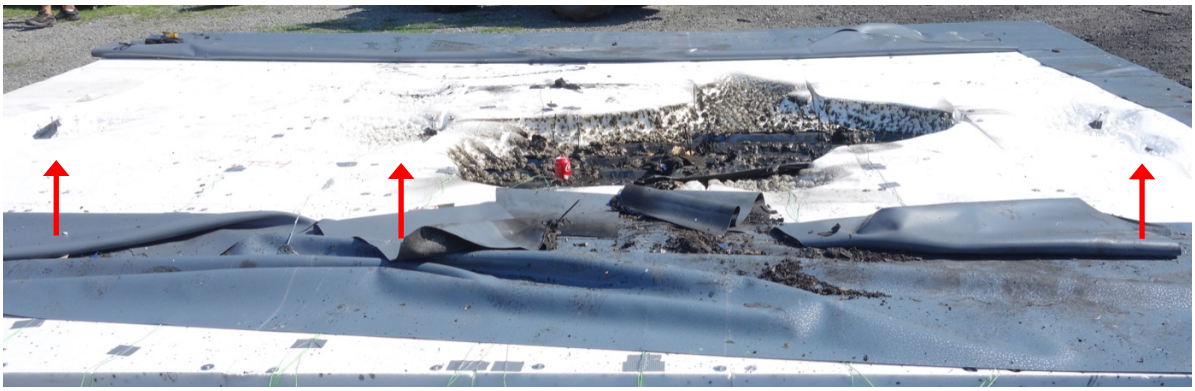

a) From experiment T3 (PIR insulation). The damaged area was limited due to extinguishment by fire fighters. Notice; 1) the sooty sides of the EPS insulation and the carbonised area in the centre of the hole. 2) The melted areas above the three red arrows. The observed smoke production and the recorded temperatures also support the postulation that the EPS ignited.

b) From T4 (mineral wool). The absence of soot on the EPS insulation, combined with the lack of smoke observations and the low recorded temperatures, suggests that no ignition occurred, and the damage of the EPS only happened due to the conductive heat transfer through the mineral wool.

Figure 14 – Overview of the damaged existing roof construction (layer C in Fig. 2) in a) experiment T3 (PIR insulation) and b) experiment T4 (Mineral wool). The red can was placed below the point of ignition in both pictures.

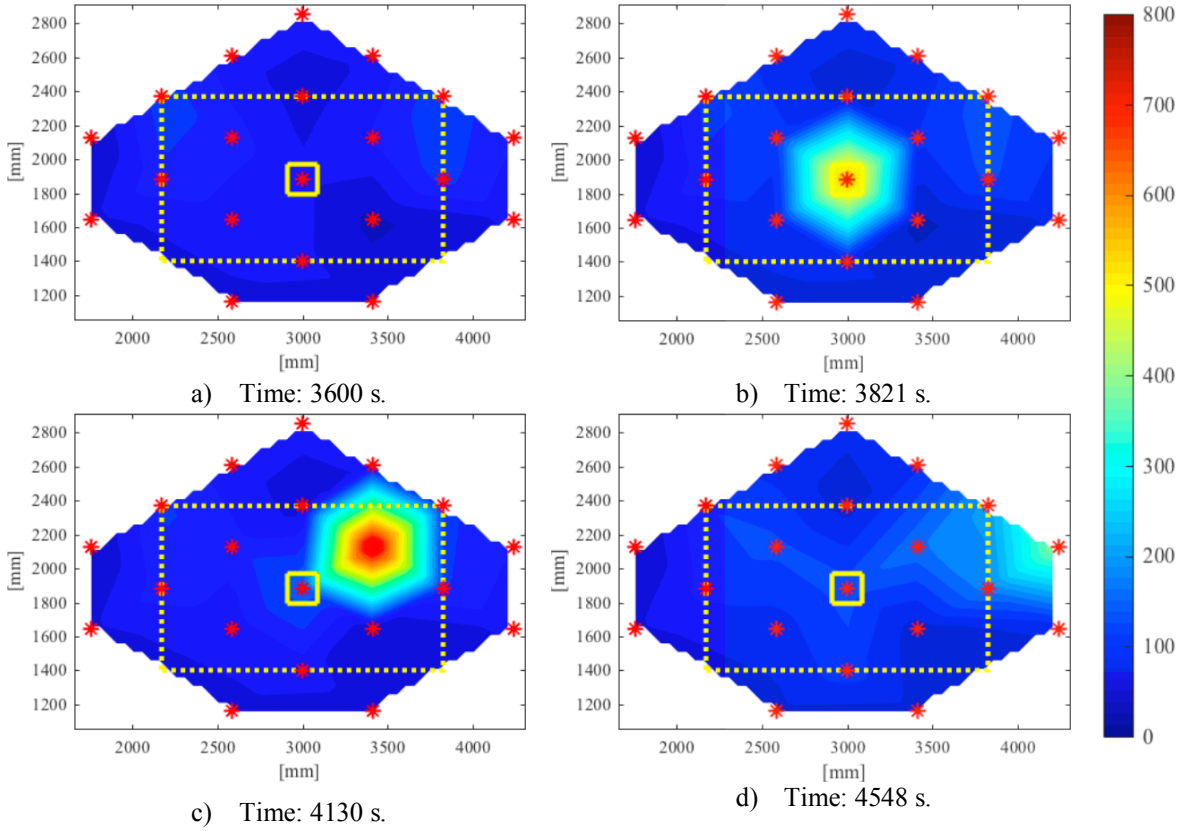

Figure 15 – T3. Development of the temperature underneath the PIR insulation in experiment T3. The different colours define the temperature in °C. The solid yellow line marks the point of ignition and the dotted yellow line indicates the edges of the PV placed above the point of ignition. The functional thermocouples are marked with red dots.

3.5 Development of temperature underneath the mitigation layers

Contour plots in Figs. 15 and 16 indicate the development of temperature on top of the EPS insulation at four (not-equivalent) instances for experiments T3 and T4. Although the contour plots in Figs. 15 and 16 only consists of four snapshots of the temperature development in experiment T3 and T4, they do indicate the main features for each test. According to the Ignition Handbook [29], piloted ignition for flame retarded EPS occurs at 366°C – 405°C and auto-ignition at 470°C. These temperatures were only measured in experiment T3 due to the earlier mentioned thermal degradation and penetration of the PIR insulation. Until the penetration of the PIR insulation, which occurs after 63 minutes, the maximum temperature below the mitigation layer in experiment T3 was 175°C. Compared to the maximum measured temperature of 243°C underneath the mineral wool in experiment T4, the temperature was significantly lower. But it is noteworthy that the maximum temperatures were more than 100°C below the minimum temperature for piloted ignition.

The maximum temperature for experiment T4 occurs 34 minutes after the ignition, whereupon the temperature decreases, due to the lack of combustible materials on top of the construction, as seen from Fig. 16 d. In Fig. 15 the temperature is plotted after the penetration of the PIR insulation and indicates how the warmest area is travelling within the EPS insulation. The hottest area in Fig. 14 is moving from the point of ignition above thermocouple 10 (Fig. 15 a), towards thermocouple 15 (Fig. 15 b) and 13 (Fig. 15 c). None of the plotted temperatures in experiment T4 exceeds the above-mentioned temperature for piloted ignition of flame retarded EPS [29]. The lack of high temperatures is made on purpose to make a similar scaling between Figs. 15 and 16. Furthermore, the high temperatures only occurred for a few minutes near each thermocouple due to the limited mass of the combustible EPS insulation, as seen from Fig. 17. The short duration of the high temperatures in Fig. 17 indicates ignition and combustion of the EPS insulation. Due to the significant temperature increase and smoke

development, it was decided to extinguish the experiment after 75 minutes, as this also enabled examination of the post-fire damages to the roof construction.

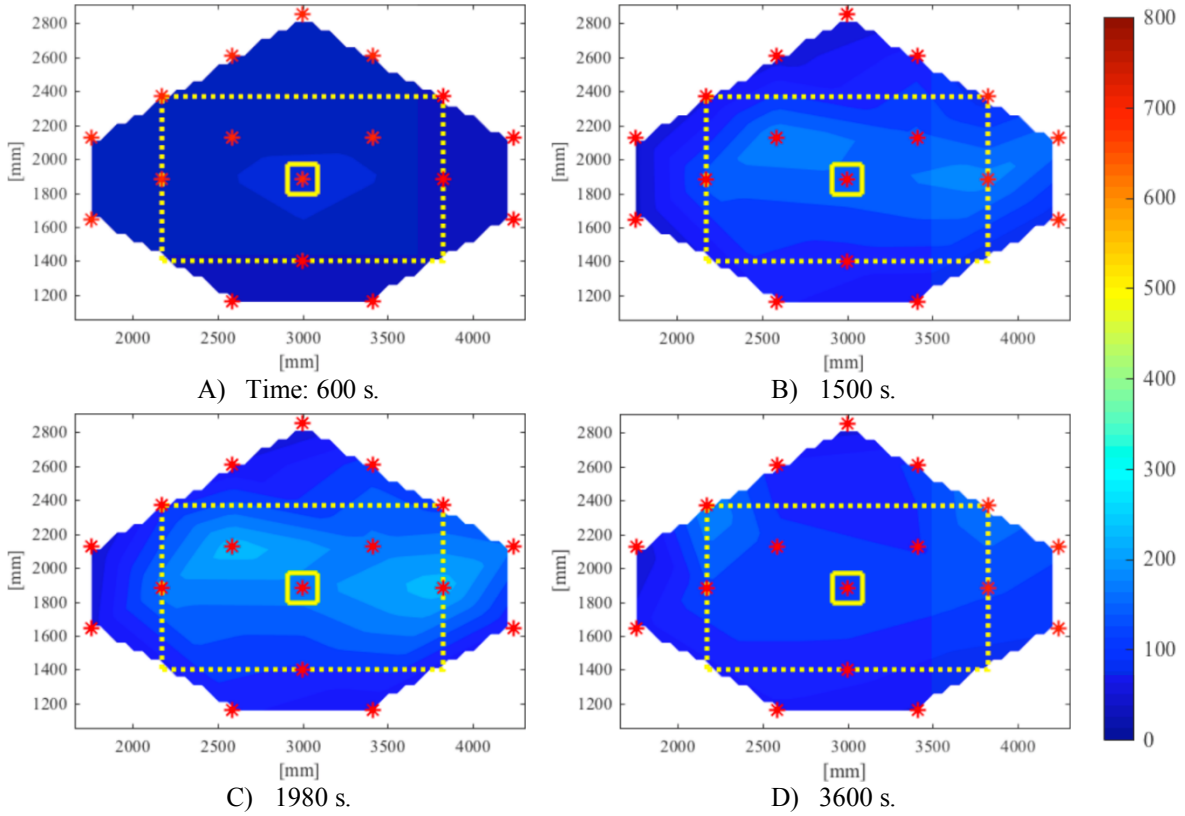

Figure 16 – T4. Development of the temperature underneath the mineral wool in experiment T4. The different colours define the temperature in °C. The solid yellow line marks the point of ignition and the dotted yellow line indicates the edges of the PV placed above the point of ignition. The functional thermocouples are marked with red dots.

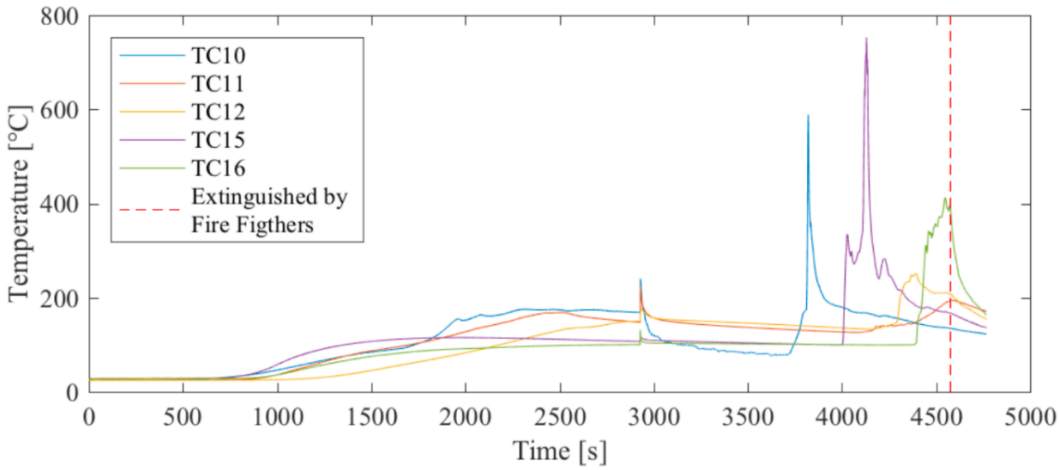

Figure 17 - T3. Temperatures measured in selected thermocouples (TC). The number of the TC refers to the position seen in Fig. 6.

4. Conclusion

Four experiments with PV panel arrays on flat roof constructions were carried out to examine the fire dynamics behaviour and flame spread on the substrate underneath the panels. In all experiments a small wood crib was used as ignition source and it was tested if a mitigation layer of either 40 mm PIR insulation or 30 mm mineral wool could prevent downwards spread of fire.

The four experiments covered herein demonstrated, that the spread area of fire on a roof construction with PV arrays were limited by the area of the arrays. In all four tests, the fire propagated underneath all panels, uninfluenced by differences in the wind conditions (no wind and moderate wind). Furthermore, the limited propagation outside the PV array was not influenced by the type of mitigation layer and no sustained fire occurred, even with a concurrent wind flow. These results are in accordance with lab-scale studies focusing on the re-radiation cause by PV panels in a fire [19] and confirm that it is the changed fire dynamic scenario that is the main cause for fire spread over the membrane, and not the fire load of the panels, the wind or the low critical heat flux of the membrane.

40 mm PIR insulation (T1 and T3) and 30 mm mineral wool (T2(w/alu) and T4) were tested as mitigation layers to protect a subjacent layer of expanded polystyrene (EPS) from ignition, which partially succeeded for both solutions within an hour after ignition. Where the ignition of the EPS insulation in experiment T1 may have occurred due to ignition from the side of the mock-up, it was not the case in test T3. After one hour and three minutes, the mechanical properties of the PIR insulation in experiment T3 failed, the material was penetrated by the fire, and the EPS insulation was ignited. In both experiments with PIR insulation it was necessary to extinguish the fire by assistance from the fire fighters, indicating that a fire in the EPS insulation is sustainable in case of ignition, due to the fuel/air-ratio of the material. Contrary to experiments T1 and T3, the mineral wool in experiments T2 and T4 remained stable throughout the experiments. The mechanical stability and the maximum measured temperature of 243°C prevented an ignition of the EPS insulation.

The obtained results provide an increased understanding of the fire related risk introduced by the installation of PV arrays. The results indicate that the geometry of the PV installations has a significant influence on the propagation. The fire related risk of PV panels is thereby not only dependent on the new installation, - but also on the materials in the existing roof construction. Although the roofing membrane was classified as B_{ROOF} (t2) according to EN 13501, the fire propagated quickly due to the additional contribution of heat reflected by the PV panels. Solving the issue will require further studies within multiple fields of fire safety engineering, such as understanding; 1) how the materials used on existing roof constructions react to fire, when they are exposed to the abovementioned combined heat flux; 2) how the design of the PV installations, such as elevation and inclination of the panels and distance between individual arrays, influences the spread of fire; 3) how the components related to the PV installation, such as the mounting system, reacts to fire; and finally 4) how the spread of fire is affected by different weather conditions such as wind, which could accelerate the propagation even further.

In brief, these full-scale experiments confirm that an initial fire underneath a PV installation can transform into a hazardous scenario due to the changed fire dynamics of the existing roof, where combustible construction materials can become fuel loads and thereby increase the fire risk through increased consequences. Combined with the fact that introducing PV panels increases the probability of a fire, the overall risk in terms of probability times consequence can increase significantly unless properly managed through the use of the proper fire mitigation and fire management solutions.

References

1. Masson G, Kaizuka I, Brunisholz M (2018) 2017 Snapshot of Global Photovoltaic Markets. IEA International Energy Agency. ISBN 978-3-906042-72-5. http://www.iea-pvps.org/fileadmin/dam/public/report/statistics/IEA-PVPS_-_A_Snapshot_of_Global_PV_-_1992-2017.pdfAccessed 3 August 2018.

2. SEIA Solar Energy Industries Association (2017) Solar Means Business 2016 – Tracking Solar Adoption by America's Top Companies, http://www.seia.org/research-resources/solar-means-business-2016. Accessed 12 April 2018.

3. SEIA Solar Energy Industries Association (2017) Solar Industry Data Solar Industry Growing at Record Pace, http://www.seia.org/research-resources/solar-industry-data. Accessed 12 April 2018.

4. Fiorentini L, Marmo L, Danzi E, Puccia V (2015) Fires in photovoltaic systems: Lessons learned from fire investigations in Italy. SFPE Emerging Trends Enewsletter. http://www.sfpe.org/?page=FPE_ET_Issue_99&hhSearchTerms="issue+and+99, Accessed 21 June 2017.

5. Cancelliere P (2014) PV electrical plants fire risk assessment and mitigation according to the Italian national fire services guidelines. Fire Mater 40:355–367. https://doi.org/10.1002/fam.2290

6. Zhao Y, de Palma JF, Mosesian J, Lyons R, Lehman B (2013) Line–line fault analysis and protection challenges in solar photovoltaic arrays, IEEE Transactions on Industrial Electronics, 60:3784-3795, https://doi.org/10.1109/TIE.2012.2205355

7. Brooks B (2012) The ground-fault protection blind spot: A safety concern for larger photovoltaic systems in the United States. Solar American Board for Codes and Standards. http://www.solarabcs.org/about/publications/reports/blindspot/, Accessed 12 April 2018.

8. Pandian A, Bansal K, Thiruvadigal DJ, Sakthivel S (2015) Fire hazards and overheating caused by shading faults on photo voltaic solar panel, Fire Technol 52(2)349-364. https://doi.org/10.1007/s10694-015-0509-7

9. Wohlgemuth JH, Kurtz SR (2012) How can we make PV panels safer? In Proc. 38th IEEE Photovoltaic Spec. Conf. pp. 3162-3165. https://doi.org/10.1109/PVSC.2012.6318250

10. Grant CC (2010) Fire fighter safety and emergency response for solar power systems. The Fire Protection Research Foundation. https://www.nfpa.org/-/media/Files/News-and-Research/Resources/Research-Foundation/Research-Foundation-reports/For-emergency-responders/RFFirefighterTacticsSolarPowerRevised.ashx?la=en. Accessed 12 April 2018.

11. Backstrom B, Tabaddor M (2009) Effect of Rack Mounted Photovoltaic Modules on the Fire Classification Rating of Roofing Assemblies, UL Underwriters Laboratories. http://www.solarabcs.org/current-issues/docs/UL_Report_PV_Roof_Flammability_Experiments_11-30-10.pdf. Accessed 12 April 2018.

12. Backstrom B, Sloan D (2012) Effect of Rack Mounted Photovoltaic Modules on the Fire Classification Rating of Roofing Assemblies – Phase 2, UL Underwriters' Laboratories. http://www.solarabcs.org/current-issues/docs/UL_Report_Phase2_1-30-12.pdf. Accessed 12 April 2018.

13. Backstrom B, Sloan D. (2012) Report of Experiments of Minimum Gap and Flashing for Rack Mounted Photovoltaic Modules – Phase 4, UL Underwriters Laboratories. http://www.solarabcs.org/current-issues/docs/UL_Report_Gap_and_Flashing_Exps_3-29-12.pdf. Accessed 12 April 2018.

14. Backstrom B, Sloan D (2012) Characterization of Photovoltaic Materials – Critical Flux for Ignition/Propagation Phase 3, UL Underwriters Laboratories. http://www.solarabcs.org/current-issues/docs/UL_Report_Critical_Flux_Experiments_1-16-12.pdf. Accessed 12 April 2018.

15. Backstrom B, Tabaddor M (2009) Effect of Rack Mounted Photovoltaic Modules on the Fire Classification Rating of Roofing Assemblies – Demonstration of Mitigation Concepts. UL Underwriters Laboratories, http://www.solarabcs.org/current-issues/docs/UL_Report_PV_and_Roof_Flammability_Mitigation_2-10-10.pdf. Accessed 12 April 2018.

16. Backstrom B, Sloan D (2012) Considerations of Module Position on Roof Deck during Spread of Flame Tests – Phase 5, UL Underwriters Laboratories. http://www.solarabcs.org/current-issues/docs/UL_Report_Module_Reposition_Experiments_7-24-12.pdf. Accessed 12 April 2018.

17. Backstrom B (2013) Validation of Roof Configuration 2 Experiments Project 9. UL Underwriters Laboratories, http://www.solarabcs.org/current-issues/docs/Validation_of_Roof_Configuration_2_Experiments.pdf. Accessed 12 April 2018.

18. Cancelliere P, Liciotti C (2014) Fire Behaviour and Performance of Photovoltaic Module Backsheets. Fire Technol 52(2)333-348. https://doi.org/10.1007/s10694-014-0449-7.

19. Kristensen JS, Merci B, Jomaas G (2018) Fire-induced Re-radiation underneath Photovoltaic Arrays on Flat Roofs. Fire Mater 2018;42:316-323. https://doi.org/10.1002/fam.2494.

20. Backstrom R, Dini D (2012), Firefighter safety and photovoltaic installations research project, Tech. Rep., Under writers Laboratories Inc., https://www.scopus.com/record/display.uri?eid=2-s2.0-84872120047&origin=inward&txGid=127f9641ea664c227649bacf72d6aed3. Accessed 12 June 2018.

21. Ramsdal R (2017), Brannsjef mener solceller kompliserte Asko-brannen, Teknisk Ukeblad TU Byg. https://www.tu.no/artikler/brannsjef-mener-solceller-kompliserte-asko-brannen-det-er-sol-grunder-rivende-uenig-i/382843, Accessed 6 August 2018.

22. Rogers J (2017), Solar panel fire fears after panels ignite in new block with thousands possibly at risk, Express, https://www.express.co.uk/news/uk/826553/Solar-panel-fire-fears-BRE-flats-east-London-Bethnal-Green, Accessed 6 August 2018.

23. Kristensen JS (2015) Fire Risk Assessment of Solar Cell Array Installations on Large Buildings: How to Protect the Building in Case of Fire? Tech. Rep., Technical University of Denmark (DTU), Department of Civil Engineering, Kgs. Lyngby, Denmark.

24. Zhou L, Fernandez-Pello AC (1991) Concurrent turbulent flame spread. Symp. Int. Combust. Proc. 1991;23:1709-1714. https://doi.org/10.1016/S0082-0784(06)80446-7.

25. Zhou L, Fernandez-Pello AC, Cheng R (1990) Flame spread in an opposed turbulent flow. Combust. Flame 1990;81:40-49. https://doi.org/10.1016/0010-2180(90)90068-3.

26. Zhang X, Tao H, Xu W, Liu X, Li X, Zhang X, Hu L (2017) Flame extension lengths beneath an inclined ceiling induced by rectangular-source fires, Combust. Flame 2017;176:349-357. https://doi.org/10.1016/j.combustflame.2016.11.004

27. Qiu A, Hu L, Chen LF, Carvel RO (2018) Flame extension lengths beneath a confined ceiling induced by fire in a channel with longitudinal air flow, Fire Saf J 2018:97:29-43. https://doi.org/10.1016/j.firesaf.2018.02.003

28. McAllister S, Finney M (2013) Effect of crib dimensions on burning rate. In: Bradley D, Makhviladze G, Molkov V, Sunderland P, Tamanini F (eds) Proc. of the seventh international seminar on fire & explosion hazards (ISFEH7). https://doi.org/10.3850/978-981-07-5936-0_08-02.

29. Babrauskas V (2014) Ignition Handbook, Fire Science Publishers. ISBN 0-9728111-3-3, p. 1069